

5  
NP-6976

NP  
NSA

MASTER

Copy No. 66  
of 80 copies

TECHNICAL REPORT 62

on

Contract NObs-65426

Index No. NS-200-021

~~PARTIAL FILM BOILING WITH WATER~~

~~AT 2000 PSIG~~

~~IN A ROUND VERTICAL TUBE~~

J. B. McDonough

W. Milich

E. C. King

October 8, 1958

**MSA** Research Corporation

*Subsidiary of Mine Safety Appliances Company*

Callery, Pennsylvania

## **DISCLAIMER**

**This report was prepared as an account of work sponsored by an agency of the United States Government. Neither the United States Government nor any agency Thereof, nor any of their employees, makes any warranty, express or implied, or assumes any legal liability or responsibility for the accuracy, completeness, or usefulness of any information, apparatus, product, or process disclosed, or represents that its use would not infringe privately owned rights. Reference herein to any specific commercial product, process, or service by trade name, trademark, manufacturer, or otherwise does not necessarily constitute or imply its endorsement, recommendation, or favoring by the United States Government or any agency thereof. The views and opinions of authors expressed herein do not necessarily state or reflect those of the United States Government or any agency thereof.**

## **DISCLAIMER**

**Portions of this document may be illegible in electronic image products. Images are produced from the best available original document.**

File No. 1610

TECHNICAL REPORT 62

on

Contract NObs-65426  
Index No. NS-200-021

PARTIAL FILM BOILING WITH WATER AT 2000 PSIG  
IN A ROUND VERTICAL TUBE

J. B. McDonough  
W. Milich  
E. C. King

October 8, 1958

Signed: R. C. Werner  
R. C. Werner  
Operations Manager

Approved: C. B. Jackson  
C. B. Jackson  
Vice President  
Director of Research

MSA RESEARCH CORPORATION  
Callery, Pennsylvania

## TABLE OF CONTENTS

	Page No.
ACKNOWLEDGEMENT	i
ABSTRACT	ii
LIST OF FIGURES	iii
LIST OF TABLES	iv
1 INTRODUCTION	1
2 APPARATUS	1
3 TEST PROCEDURE	3
4 CALCULATING PROCEDURE	4
5 DISCUSSION OF RESULTS	5
6 ACCURACY OF DATA AND RESULTS	7
7 CONCLUSIONS	9
8 NOMENCLATURE FOR TEXT AND APPENDIX I	11
9 LITERATURE CITED AND REFERENCES	13
10 APPENDICES	14
APPENDIX I FIGURES AND TABLES	15
APPENDIX II DETERMINATION OF THE LOCAL NUSSELT NUMBER FOR FLOW THROUGH AN ANNULUS WITH HEAT TRANSFER FROM ONE SIDE	33

## ACKNOWLEDGEMENT

The authors wish to thank Messrs. S. J. Green and M. Troy of Westinghouse, Atomic Power Division, Bettis Plant, for their help and contribution in the performance of this work.

## ABSTRACT

A study of the partial film boiling region of water at 2000 psig was made in a 1/4 in. OD vertical Inconel-X tube, 0.152 in. ID x 12-1/2 in. long. The water parameters were: mass flow rates approximately  $0.4 \times 10^6$  to  $1.5 \times 10^6$  lb/hr-sq ft, at inlet enthalpies of  $\sim 377$  to 614 Btu/lb. NaK, a liquid metal, was used as the heating medium.

The wall temperatures measured in the nucleate boiling region agreed within approximately  $\pm 10^{\circ}\text{F}$  of Jens & Lottes correlation. The burnout heat flux results reported agree within approximately  $\pm 25\%$  of WAPD (Bettis Plant) correlation. The film boiling data does not appear to yield to correlation over the range investigated in this experiment. The partial film boiling coefficients found in this experiment range from approximately 100 to 10,000 Btu/hr sq ft- $^{\circ}\text{F}$ .

Future test programs will furnish data in the partial film boiling region at elevated pressures of 2000, 1200 and 800 psig.

## LIST OF FIGURES

	Page No.
Fig. 1 Flow Diagram to Study Film Boiling of Water Inside a Tube	16
Fig. 2 Heat Exchanger for Water Burnout Loop	17
Fig. 3 NaK Bulk Temperature Vs Distance Along Exchanger	18
Fig. 4 Temperature Vs Distance Along Exchanger - Run 6-2	19
Fig. 5 Heat Flux Vs Distance Along Exchanger Run 6-2	20
Fig. 6 Heat Flux Vs Wall Temperature - Run 6-2	21
Fig. 7 Enthalpy Vs Wall Temperature - Run 6-2	22
Fig. 8 Water Coefficient Vs Wall Temperature Run 6-2	23
Fig. 9 Partial Film Boiling Coefficients Vs $T_w - T_s$	24
Fig. 10 Results of Variable Heat Flux on NaK Conductance	25
Fig. 11 NaK Bulk Temperature Vs Distance Along Exchanger - Run 15-2	26

## LIST OF TABLES

	Page No.
Table 1      Heat Transfer Coefficients of Water Inside Tube 0.152 ID x 12-1/2 in. In Length	27 - 31
Table 2      Comparison of MSAR Data and WAPD Burnout Flux	32
Table 3      Heat Fluxes for Run 11-2	38
Table 4      Evaluation of Integral for Run 11-2	39
Table 5      Results Showing the Effect of Variable Heat Flux on the Local NaK Conductance	41
Table 6      Results on Corrected NaK Conductance	42

Partial Film Boiling with Water at 2000 psig  
in a Round Vertical Tube

J. B. McDonough  
W. Milich  
E. C. King

1 INTRODUCTION

One of the major limitations on the power output of a pressurized water nuclear reactor is the heat transfer burnout.\* This occurs when the heat transfer surface of the fuel element becomes steam blanketed by an unstable, irregular film which is in violent motion. Presence of the vapor on a heat transfer surface causes the heat transfer coefficient to drop and a rapid rise in fuel element temperature. This temperature increase could result in overheating and possible failure of the fuel element and the release of fission products into the reactor. Consideration is being given at the present time to operate nuclear reactors, following accidental conditions (rod jump, loss of coolant and loss of coolant flow), for a short period (order of seconds) of time in the partial film boiling region.

The present thermal design margin in a nuclear reactor is based on a no-burnout criteria, consequently the transient operation of the reactor is designed to scram in a fraction of seconds. Before the present thermal design procedure is changed it becomes necessary to know the heat transfer coefficient in the partial film boiling region.

The purpose of this investigation was to provide the necessary data to estimate heat transfer coefficients in the partial film boiling region at an elevated pressure of 2000 psig.

2 APPARATUS

NaK Side

A schematic diagram of the experimental system is shown in Fig. 1. An EM pump was used to circulate the NaK past a magnetic flowmeter, up through a 25 KW electric immersion heater, past an expansion tank, down through the shell side of the test section, past a second magnetic flowmeter and back into the pump. The main piping was constructed of 1 in. Sch 80, Type 316 ss. All fittings were Sch 80, socket welded Type 316 ss. Heat was supplied to the NaK system by 6 calrod immersion type heaters with a total rating of 21 KW. The heaters were manually controlled by a bank of 6 high powerstats. The system contained approximately 35 lb of NaK.

---

\* Burnout is defined, in this report, as the departure in magnitude from the uniform wall temperature ( $\sim 642^{\circ}\text{F}$ ) in the nucleate boiling region.

(56% K) and the flow was measured at two different locations by magnetic flowmeters. The flowmeters were calibrated over their range to be accurate to within 2% of the instantaneous flow reading.

#### Water Side

A Westinghouse 30 gal/min canned rotor pump was used to circulate the water (see Fig. 1). The water was pumped through 3 flowmeters connected in series, through a 25 KW pre-heater, up through the tube side of the test section, through the cooler, past the pressurizer, and back again into the pump. To maintain water purity, some water flow was by-passed at the pump discharge, through an economizer, a cooler, down through a demineralizer, and back into the suction side of the pump. The flow was normally measured by one of three Fisher and Porter rotameters connected in parallel. These were in series with an orifice and venturi meter used for flow measurement during the period of heat transfer data collection.

The main water piping was constructed of 1 in. Sch 80 Type 304 ss pipe. The fittings were Sch 80 socket welded Type 304 ss and the main system valves were Powell globe with Type 316 ss cast bodies with Stellite seats and plugs and Teflon packing.

The surge tank, used to degas the water and pressurize the system, was equipped with 8 calrod immersion type heaters rated at 30 KW. Six of the heaters were manually controlled and the other two operated automatically to control the pressure within  $\pm 25$  psi. A fisher and Porter liquid level controller operated the Hills McCanna makeup pump. Two mercoid switches, incorporated as a safety feature, were wired for high and low level control which would automatically shut the system down at either level.

The de-ionizer, used to maintain the water purity at approximately 2 meg-ohm-centimeters, contained a 3-1/2 in. diam x 36 in. bed of Rohm and Hass mixture AB resin.

The pre-heaters were a combination of cast in bronze heaters and cal-rods. Their function was to control the water inlet temperature to the test section. The total capacity of the pre-heaters was 25 KW with about 75% of the power controlled direct and 25% by a manually operated powerstat.

The water to air cooler fabricated by Griscom-Russell was designed to remove 45,000 Btu/hr, which was the maximum heat input in the test section.

Flow was measured by an orifice meter and a venturi meter connected in series with three parallel Fisher and Porter rotameters. The orifice and venturi meters were calibrated over their range to be accurate to within 2% of the instantaneous flow reading. The rotameters were guaranteed for 2% accuracy at top scale reading and 20% at bottom scale readings.

### Thermocouples

The bulk temperatures of both the NaK and the water streams were measured by two thermocouples at the exits and entrances of the test section. Chromel-Alumel and Iron Constantan thermocouples were used on the NaK and water sides respectively. These thermocouples were insulated and inserted into 1/8 in. stainless steel wells. To minimize axial conduction, one thermocouple in each set had at least a 5 in. length immersed in an isothermal region. Mixing chambers were placed at the exits and entrances of the test section to secure complete mixing. In addition to the bulk fluid thermocouples, 40 external thermocouples (station thermocouples) were silver soldered on the outside wall of the test section. To check the concentricity of the tube and to obtain more data in the peak heat flux region, twenty of the 40 thermocouples were added toward the end of the test program. See Fig. 2 for orientation of these thermocouples. The bulk thermocouples were calibrated over the temperature range covered in this experiment. An ice bath was used as a cold-junction reference and all thermocouples were read on a self balancing Brown precision potentiometer.

The test section (see Fig. 2) was designed in an "L" shape to take care of differential expansion between the tube and the shell. The tube was 0.152 in. ID x 0.25 in. OD x 12.5 in. heated length. The tube material was Inconel-X which has a high strength and good corrosion resistance at elevated temperatures.

### 3 TEST PROCEDURE

In the preliminary tests the tube wall temperatures were determined from the station thermocouples located on the outside wall of the exchanger. A calibration of these thermocouples was obtained by flowing NaK in the annulus without the test fluid and plotting station thermocouples versus NaK bulk temperature. The bulk temperatures across the tube were corrected for radiation losses.

Before the film boiling tests were run, it was necessary to establish a calibrated forced convection annular coefficient equation for NaK. A series of tests were run using NaK on both sides of the test section. The results indicate the annular coefficient could be estimated by the following equation:

$$\frac{h_{NaK} D_{eq}}{k} = 4.9 + 0.025 \left( \frac{D_{eq} u \rho C_p}{k} \right)^{0.8} \quad (1)$$

Lyon's<sup>11\*</sup> equation was used for evaluation of the coefficients on the inner tube surface.

---

\* Superscripts refer to similarly numbered entries in the Bibliography section.

Runs were made with water in the forced-convection region to check the NaK coefficients predicted by equation (1). The experimental results agreed within 7% of the estimated values obtained from equation (1). The Dittus-Boelter<sup>1</sup> equation was used to determine the forced-convection film coefficients for water.

Before starting the final test program the loop was filled with demineralized water and degassed for approximately 5 hr until the oxygen content was 0.25 ppm as determined by the Winkler Method<sup>2</sup>. Some water was passed through the ion exchanger until a purity of two meg-ohm-cm was obtained. The loop was raised to the test pressure of 2000 psig; the water flow rate was fixed at a given value and the pre-heaters set to give the desired water inlet temperature. The heat was supplied to the test section from NaK flowing in the annulus until equilibrium conditions were achieved. The heat was increased step-wise to the NaK and plots of the NaK bulk temperature versus distance along the exchanger were made, Fig. 3. Three of four sets of data were recorded at each step to minimize errors in the thermocouple readings.

#### 4 CALCULATING PROCEDURE

Knowing the local distribution of the NaK bulk temperature (see Fig. 3), the local annular coefficients were calculated from equation 1. Since there was little change in the NaK physical properties along the test section, the local NaK coefficients were uniform; therefore, the average NaK coefficient was used. (See Appendix II for possible error introduced with this assumption.)

##### Local Heat Flux

The local heat flux was determined from the local slope of the NaK temperature profile (see Fig. 3) by:

$$\left(\frac{q}{A}\right)_x = \frac{w C_p}{A_z} \left(\frac{\partial t}{\partial z}\right)_x \quad \text{eq. 2}$$

##### Wall Temperature Measurement

Using the NaK annulus film coefficient, thermal conductivity (k) of the Inconel-X tube and the local heat flux, the inner tube wall temperature ( $T_w$ ) was obtained from:

$$T_w = T_{NaK} + \left[ \frac{\phi}{h_{NaK}} + \frac{\phi}{k/t} \right] \quad \text{eq. 3}$$

### Film Boiling Coefficient Measurement

With a knowledge of the NaK temperature profile (see Fig. 3), the flux distribution along the test section (Fig. 5), and the water inlet temperature, the film coefficients were determined from:

$$h_{H_2O} = \frac{\phi}{T_w - T_{water \text{ (bulk)}}} \quad \text{eq. 4}$$

### 5 DISCUSSION OF RESULTS

A typical run illustrating nucleate and partial film boiling is shown, (see Fig. 3). The lower curves (Runs 6-1 and 6-2) indicate that two phases of boiling (nucleate and partial film) were present simultaneously in different regions of the tube of the test section. Runs 6-3 and 6-4 illustrate film blanketing across the entire heat transfer surface with the early film boiling region occurring approximately at stations 12 through 13. Fig. 4 through 8 show the direct results of the experimental work for run 6-2.

The heat transfer rate associated with nucleate boiling is very high as compared to film boiling, because of the agitation by the bubble population of the water near the heating surface. The heat transfer rate associated with partial film boiling, as represented by the nearly horizontal portion (see Fig. 3) of the curves, is much lower due to the insulating vapor present on the heat transfer surface.

Fig. 4 illustrates composite plots of NaK bulk ( $T_{NaK}$ ), inner tube wall ( $T_w$ ), and water bulk ( $T_{H_2O}$ ) temperatures versus distance along the test section. The existence of the nucleate boiling region is indicated by the uniform axial water side wall temperature of  $642^\circ F$  ( $\pm 10^\circ$ ) which is in close agreement with Jens and Lottes<sup>8</sup> prediction of  $642^\circ F$ . The point of departure upward from the uniform wall temperature indicates the initiation of partial film boiling. The dotted portion at the departure represents the uncertainty of the exact position where film boiling initiation occurred. The accuracy of this point is probably within  $\pm 1/2$  in. The wall temperature curve also shows that a variation of approximately  $300^\circ F$  occurs in about 1 in. of the tube in the transition region. To increase the data and the degree of accuracy in this critical region, additional external thermouples were added toward the end of the test program. Repeat runs had been scheduled to investigate this region more thoroughly but the experiment was terminated following the test section failure during the last week of operation. A future experiment at elevated pressures of 1200 and 800 psia will also include repeat runs at the 2000 psig range.

The heat flux distribution along the test section for nucleate and partial film boiling is shown (see Fig. 5). The uncertainty of the exact burnout flux occurrence in the tube is represented by the dotted portion of the curve.

Fig. 6 shows the local heat flux distribution as a function of water side axial wall temperature. The departure in magnitude from the uniform wall temperature indicates film blanketing. One can observe that the flux in the nucleate boiling region can increase several fold without a corresponding increase in the wall temperature. The departure from the peak heat flux shows a sharp increase in the tube wall temperature with a decrease of the corresponding heat flux.

The water enthalpy distribution versus tube wall temperature for run 6-2 is shown in Fig. 7. The change in boiling regions is indicated by a departure from the uniform wall temperature. This curve is also indicative of the heat transfer rate to the water in the nucleate and film boiling regions.

Fig. 8 is a plot of local heat transfer coefficients of the water as a function of the water side tube wall temperature. The magnitude of the nucleate boiling coefficients in this particular run ranged from 2,000 to 90,000 Btu/hr-sq ft-°F. These coefficients account for the high heat transfer rate attributed to the nucleate boiling region. The change from the nucleate boiling to the film boiling region is accompanied by a decrease in the film coefficient to approximately 200 Btu/hr-sq ft-°F.

The film and nucleate boiling data are tabulated and shown in Table 1. The majority of the partial film boiling data reported were in the quality region where the enthalpy is equal to or greater than the enthalpy at the saturation temperature.

The partial film boiling coefficients follow the expected pattern, the higher the tube wall temperature the lower the coefficients. The reason for this behavior is that radiation does not play an essential role in the partial film boiling region. A decrease of the heat flux or film coefficient with a corresponding increase in tube wall temperature must be due to an increase in the thickness of the vapor film and this effect is relatively larger than the increase of the tube wall temperature. This decrease continues until stable film boiling is initiated, where radiation through the film begins to have considerable effect. Run 14-3 (Table 1) illustrates complete film boiling which is indicated by the uniform heat flux along the test section.

The film boiling data obtained in this experiment is shown graphically in Fig. 9. This plot shows the variation of the partial film boiling coefficients as a function of the wall temperature minus the saturation temperature ( $T_w - 636$ ). The partial film boiling data over the range investigated does not appear to yield to correlation on the basis of; bulk fluid conditions, velocity, channel L/D, or inlet enthalpy. A further attempt will be made to correlate these results with data obtained in future experiments at elevated pressures of 2000, 1200 and 800 psig.

The scattering in the region of high heat fluxes and low  $\Delta T$  seems to be a function of the burnout condition.

## 6 ACCURACY OF DATA AND RESULTS

The uncertainty in calculating the heat flux, which is determined from the slope of the NaK temperature profile, is approximately 15% in the nucleate boiling region. This uncertainty increases to about 25% in the partial film boiling region because of the difficulty of maintaining true equilibrium conditions. This difficulty is attributed to, the unstable phenomena of the partial film boiling region, fluctuation in power supply to immersion heaters, and the decreasing slope of the NaK temperature profile along the tube caused by the vapor film.

Analytical estimates were made on 4 typical runs to determine the effects of axial variations of heat flux on the NaK conductance. See Appendix II for results and discussion. Fig. 10 shows the results of this analysis for Run 11-2. In general, the study indicated that a serious error in the accuracy of the results can be made due to the uncertainty of the NaK conductance. This uncertainty in the NaK conductance is caused by the rapidly changing heat flux in the burnout region which causes a changing longitudinal temperature gradient in the NaK film.

The heat balances between the NaK and water checked within 6%. These balances were only checked in the sub-cooled region, because of the lack of independent measurement of the exit steam quality during the quality runs.

The burnout heat flux results (see Table 2) agree within  $\pm 25\%$  of the values predicted by a WAPD correlation<sup>5</sup> for a round vertical tube.

The tube wall temperatures in the nucleate boiling region agreed to  $\pm 10^{\circ}\text{F}$  with the Jens and Lottes<sup>8</sup> prediction of  $642^{\circ}\text{F}$ .

### Sample Calculations

Fig. 11 is the data (corrected for thermocouple calibration) plotted for Run 15-2. The plot shows the longitudinal NaK bulk temperature distribution along the shell of the test section. (See Fig. 2 for orientation of thermocouples). In the original plot approximately 70 or more data points are used, but only some typical points are shown on this plot. The curve is drawn through the data that represent the NaK bulk temperature distribution. Knowing this distribution, local NaK coefficients could be calculated. Since there was only a slight change in the physical properties the average coefficients were used.

Annular NaK Coefficient

1132 F = NaK inlet bulk temperature

883 F = NaK outlet bulk temperature

1007 F = Average NaK bulk temperature

387 lb/hr = NaK flow (measured by magnetic flowmeters)

15.8 Btu/hr-sq ft-°F/ft = Thermal conductivity (k) of  
NaK at  $T_{avg}$ 0.235 Btu/lb-°F = Specific heat ( $C_p$ ) of NaK at  $T_{avg}$ . $12.9 \times 10^{-4}$  ft<sup>2</sup> = Annular cross sectional flow area. $2.47 \times 10^{-2}$  ft = Equivalent diameter ( $D_{eq}$ )

Sub. in eq. 1

$$h = \left[ 4.9 + 0.025 \frac{(2.47 \times 10^{-2})(387)(0.235)^{0.8}}{(15.8)(12.9 \times 10^{-4})} \right] \frac{15.8}{2.47 \times 10^{-2}}$$

$$h = 3810 \text{ Btu/hr-sq ft-°F}$$

Local Heat Flux Calculation for 1 in. Using the Temperatures  
at Stations 11 and 12, Front (See Fig. 9)

1070 F = NaK bulk temperature at Station 11

1053 F = NaK bulk temperature at Station 12

0.00332 sq ft/in. = Heat transfer area (based on inside  
diameter) for 1 in.

Sub. eq. 2

$$\begin{aligned} \phi &= \frac{q}{A} = \frac{(387)(0.235)(1070-1053)}{(0.00332)(1)} \\ &= 0.464 \times 10^6 \text{ Btu/hr-sq ft} \end{aligned}$$

Doing this for each increment along the test section and plotting local heat flux  $\phi$  versus distance along test section gives the heat flux distribution along the exchanger. The heat flux distribution for Run 6-2 is shown (see Fig. 5).

Tube Wall Temperature Calculation at Station 12, Front

$0.497 \times 10^6$  Btu/hr. sq ft = Local heat flux based on  
inside area (obtained from  
plot of  $\phi$  vs distance along  
test section).

1053 F = NaK bulk temperature at Station 12

0.49 in. = Thickness of tube (L)  
 0.152 in. = ID of tube  
 0.201 in. = Average diameter of tube  
 0.25 in. = OD of tube  
 13.7 Btu/hr ft<sup>2</sup> °F = Thermal conductivity of Inconel-X  
 at average wall temperature

Sub. eq. 3

$$T_w = 1053 - \left[ \frac{(0.497 \times 10^6)(0.152)}{(3810)(0.25)} + \frac{(0.497 \times 10^6)(0.048)(0.152)}{(12)(0.201)(13.7)} \right]$$

$$T_w = 862. F$$

#### Film Boiling Coefficient at Station 12, Front

636 F = Water bulk temperature ( $T_{water}$ ) determined from heat balance

Sub. eq. 4

$$h_{H_2O} = \frac{0.497 \times 10^6}{(862 - 636)} = 2200 \text{ Btu/hr-sq ft-}^{\circ}\text{F}$$

This analysis neglects the effects due to axial conduction in the tube wall, axial conduction in the NaK stream, and axial variation of heat flux on the NaK conductance. The above analysis is based on the average tube wall thickness which was in close agreement with the log mean value used for thick wall tubes.

Analytical estimates show the first two effects to be negligible. See Appendix II for discussion of NaK conductance.

#### 7 CONCLUSION

The major aim of this experiment was to study the partial film boiling region of water and to estimate the heat transfer coefficients in this region.

Wall temperatures during local boiling with forced circulation may be predicted within approximately  $\pm 10^{\circ}\text{F}$  by using the Jens and Lottes<sup>8</sup> correlation at 2000 psig:

$$T_w - T_{sat} = \frac{60 (\phi \times 10^{-6})^{0.25}}{P/900}$$

eq. 5

Burnout flux in a forced circulating system in a round tube may be predicted within  $\pm 25\%$  of the Bettis burnout correlation<sup>5</sup>.

Correlation of the data (as presented in Fig. 11) at this time does appear feasible, however, attempts will be made again after further experimentation at lower pressures. The data shown in Fig. 9 should be of considerable value to the reactor designers since no idea as to the magnitude of the heat transfer coefficients were known before.

## 8 NOMENCLATURE FOR TEXT AND APPENDIX I

$A_z$	- Heat transfer area per unit length (sq ft)
$C_p$	- Heat capacity of NaK (Btu/lb. $^{\circ}$ F)
$D$	- Inner diameter of test section (ft)
$D_{eq}$	- Equivalent diameter of the annulus in the test section (ft)
$G$	- Water mass flow rate (lb/hr. sq ft)
$H_{H_2O}$	- Water inlet enthalpy (Btu/lb)
$H_{BO}$	- Local enthalpy of the water at burnout (Btu/lb)
$h_{H_2O}$	- Heat transfer coefficient for water (Btu/hr-sq ft- $^{\circ}$ F)
$h_{NaK}$	- Heat transfer coefficient for NaK (Btu/hr-sq ft- $^{\circ}$ F)
$k$	- Thermal conductivity (Btu/hr sq ft $^{\circ}$ F/ft)
$k/t$	- Thermal resistance of the tube wall temperature
$L$	- Length of tube from inlet to point of reference (see Fig. 2)
$P$	- Pressure (psig)
$(q/A)_x$	- Local heat flux at point x (Btu/hr sq ft)
$T_{NaK}$	- Local NaK bulk temperature $^{\circ}$ F
$T_{H_2O}$	- Local water bulk temperature $^{\circ}$ F
$T_w$	- Inner tube wall temperature $^{\circ}$ F
$T_s$	- Water saturation temperature $^{\circ}$ F
$t$	- Tube wall thickness (ft)
$(\partial t / \partial z)_x$	- Slope of NaK temperature profile ( $^{\circ}$ F/ft)
$u$	- Velocity of NaK (ft/hr)
$w$	- NaK flow (lb/hr)

## NOMENCLATURE FOR TEXT AND APPENDIX I - continued

## Greek Letters

$\phi$  - Local heat flux (Btu/hr sq ft)

$\phi_{BO}$  - Burnout heat flux (Btu/hr sq ft)

$\rho$  - Density of NaK (lb/cu ft)

## 9 LITERATURE CITED AND REFERENCES

1. Badger and McCabe, Elements of Chemical Engineering, Mc-Graw-Hill Book Company, 1936.
2. Betz, L. D. and Betz, W. H., Betz Handbook of Industrial Water Conditioning, 4th edition, Philadelphia 24, Pa.
3. Branchero, J. T., G. E. Barker, and R. H. Boll, Chemical Engineering Progress Symposium, Serial No. 17, 51, 21 (1955).
4. Bromley, L. A., Chemical Engineering Progress, 46, 221 (1950).
5. DeBortoli, R. A., S. J. Green, B. W. Le Tourneau, M. Troy and A. Weiss, "Forced Convection Heat Transfer Burnout Studies for Water in Rectangular Channels and Round Tubes at Pressures Above 500 psia", WAPD-188, October, 1958.
6. Ellion, M. E., A Study of the Mechanism of Boiling Heat Transfer, Memorandum No. 20-88, Jet Propulsion Laboratory, Pasadena, Cal.
7. Hsu, Y. Y., J. W. Westwater, AIChE Journal 4, 63 (1958).
8. Jens, W. H., Lottes, P. A., Analysis of Heat Transfer, Burnout, Pressure Drop and Density Data for High-Pressure Water, Report No. ANL-4627, Argonne National Laboratory, P.O. Box 5207, Chicago 80, Ill.
9. Kays, W. M., and W. B. Nicoll, The Influence of Non-Uniform Heat Flux on the Convection Conductances in a Nuclear Reactor, Technical Report No. 33, Stanford University, Nov. 1, 1957.
10. Kays, W. M., Report on Analysis of Film Boiling Tests, Stanford University, Cal. (1958).
11. Liquid Metals Handbook, TID 5277, Atomic Energy Commission, Department of the Navy, Washington, D. C. (1955).
12. Perkins, A. S., and J. W. Westwater, AIChE Journal 2, 471 (1956).
13. Westwater, J. W. and J. G. Santangelo, Ind. Eng. Chem. 47, 1605 (1955).

## 10 APPENDICES

**APPENDIX I****FIGURES AND TABLES**

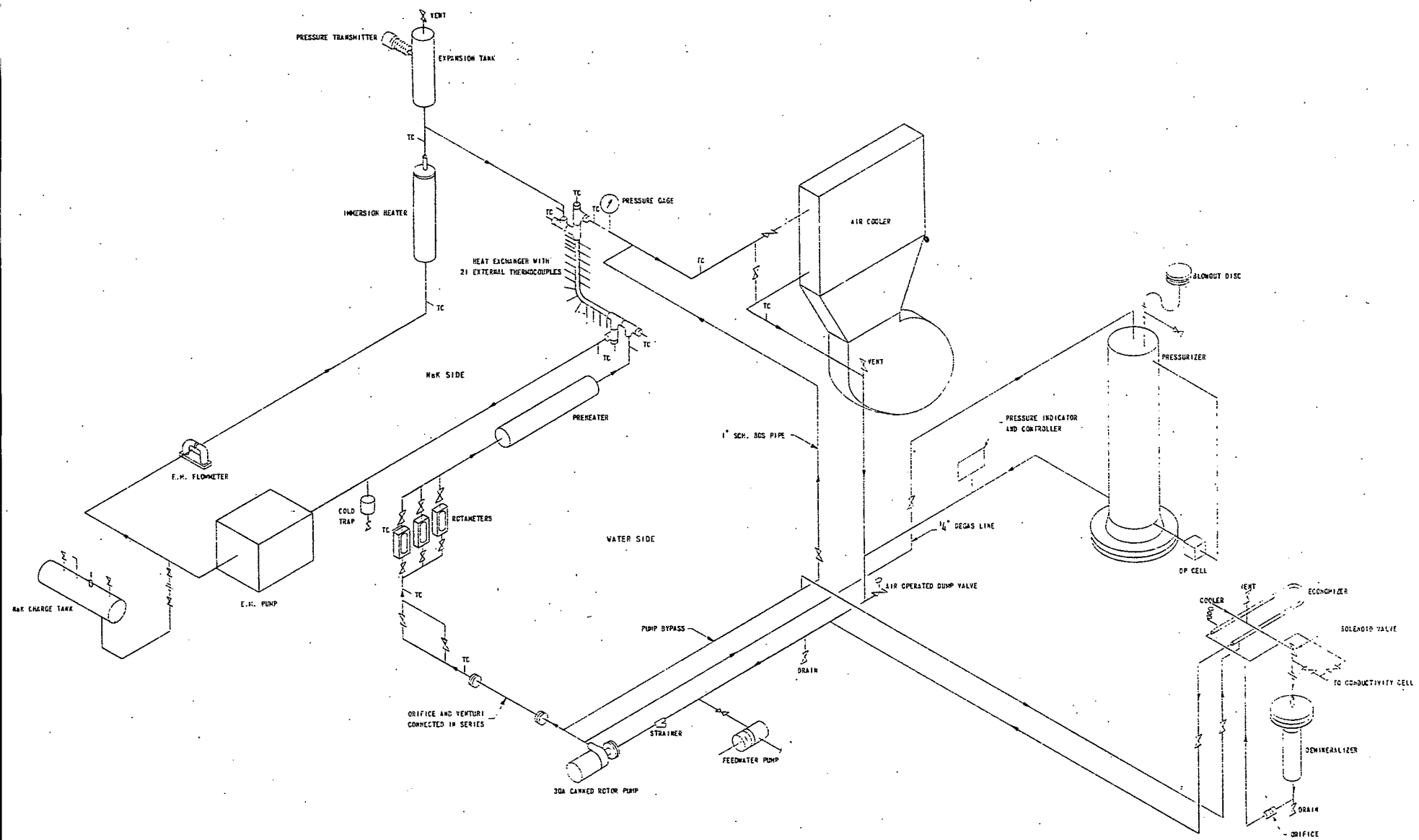


Fig. 1 - Flow Diagram to Study Film Boiling of Water Inside a Tube

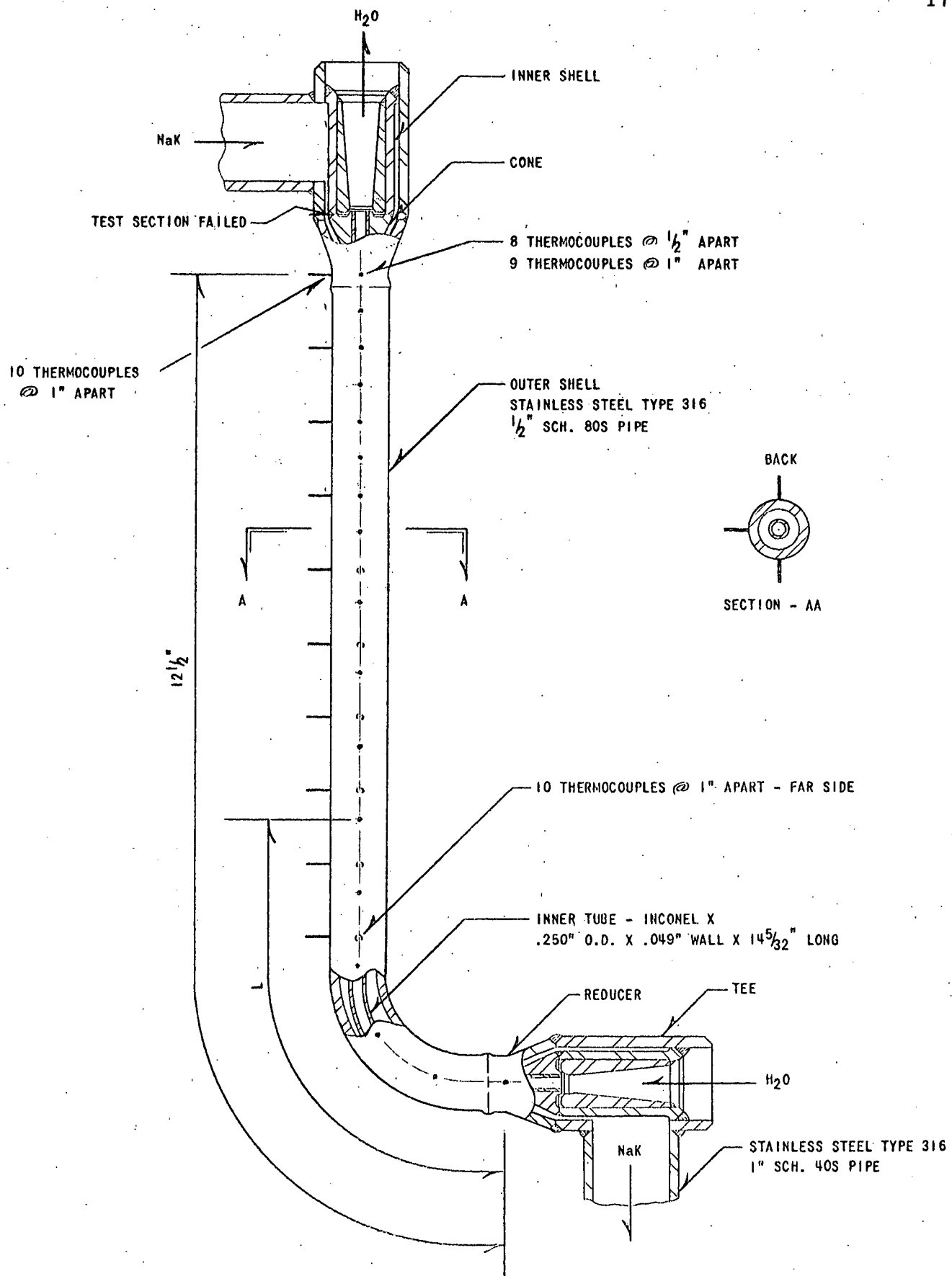


Fig. 2 - Heat Exchanger for Water Burnout Loop

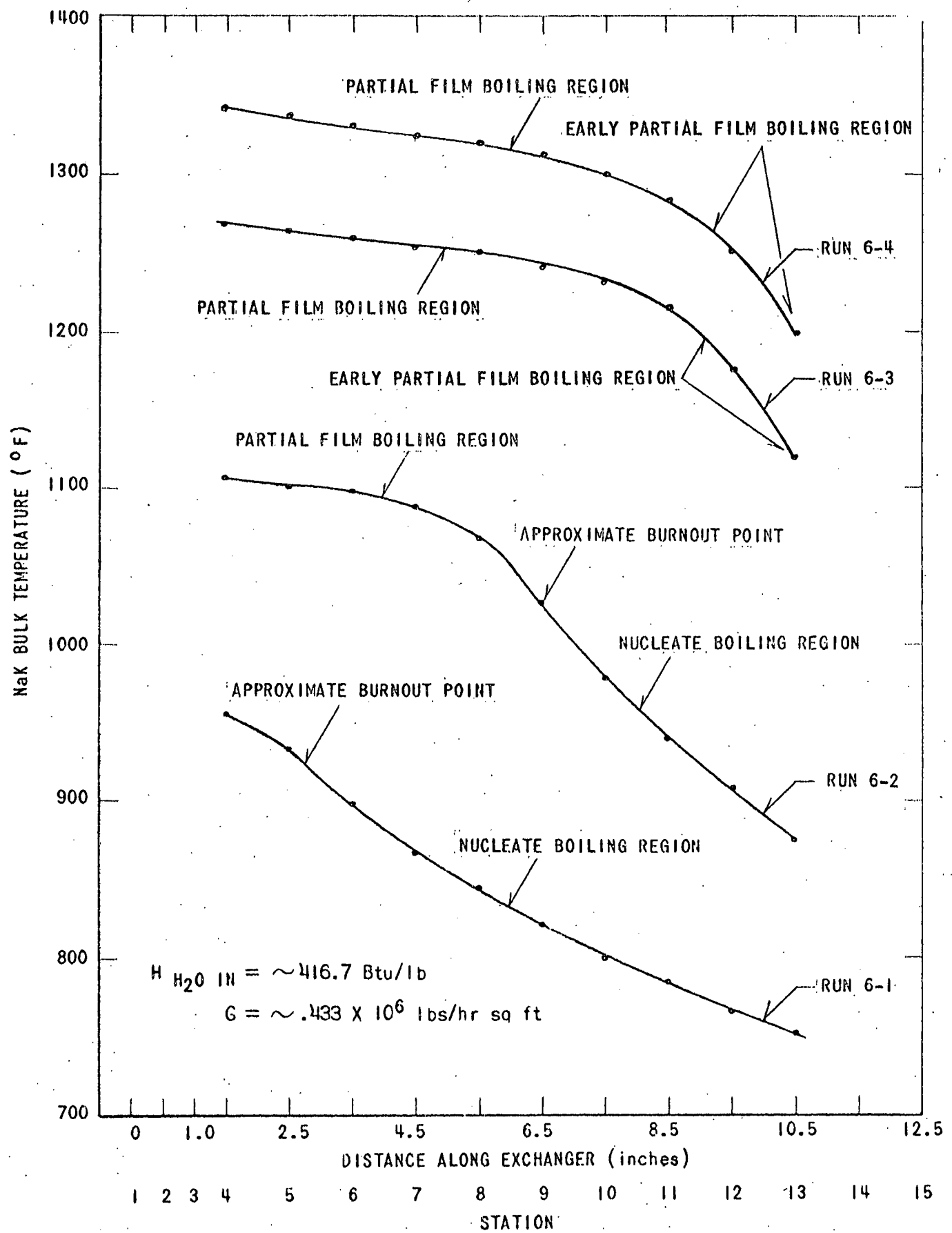


Fig. 3 - NaK Bulk Temperature vs Distance Along Exchanger

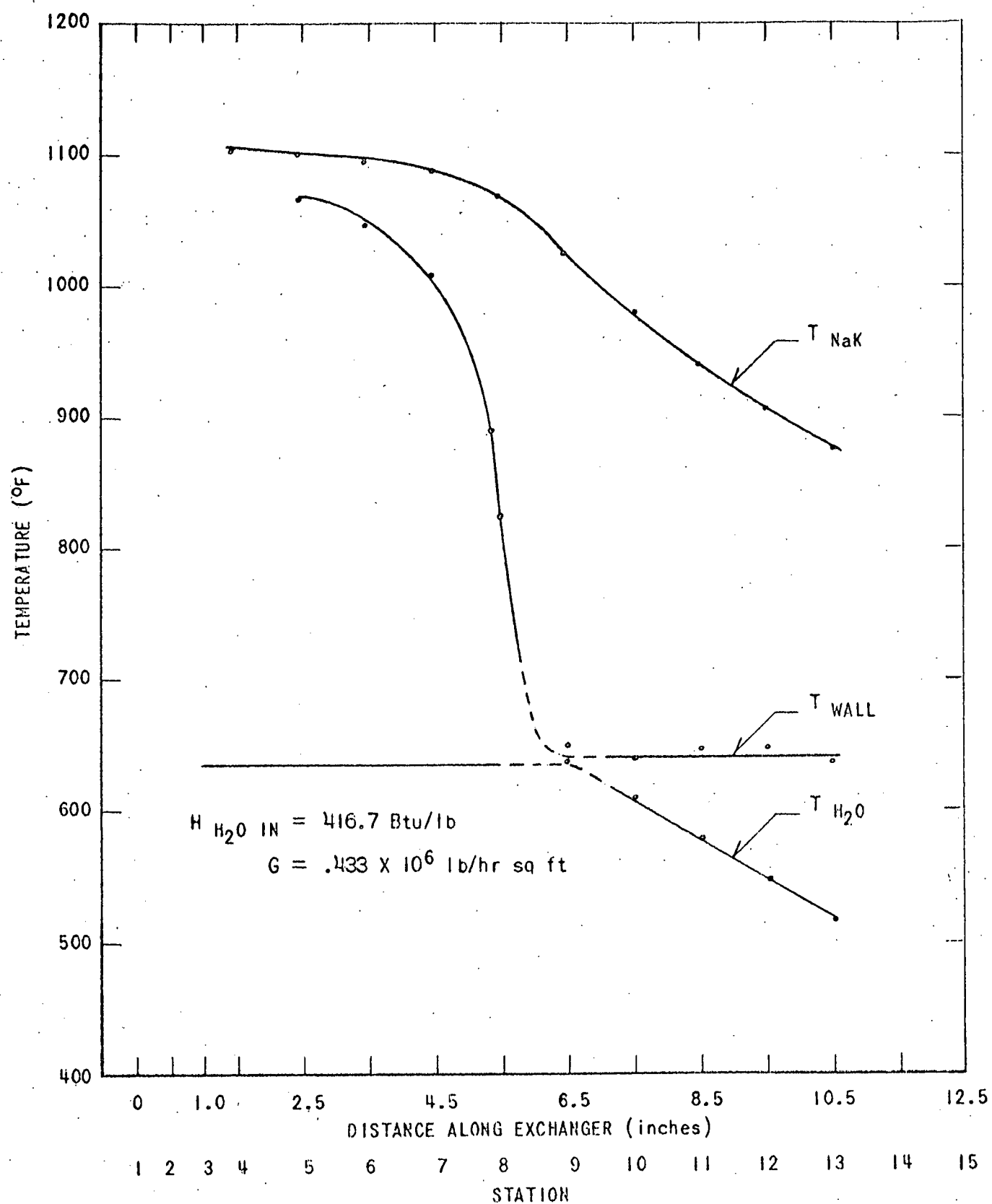


Fig. 4 - Temperature vs Distance Along Exchanger - Run 6-2

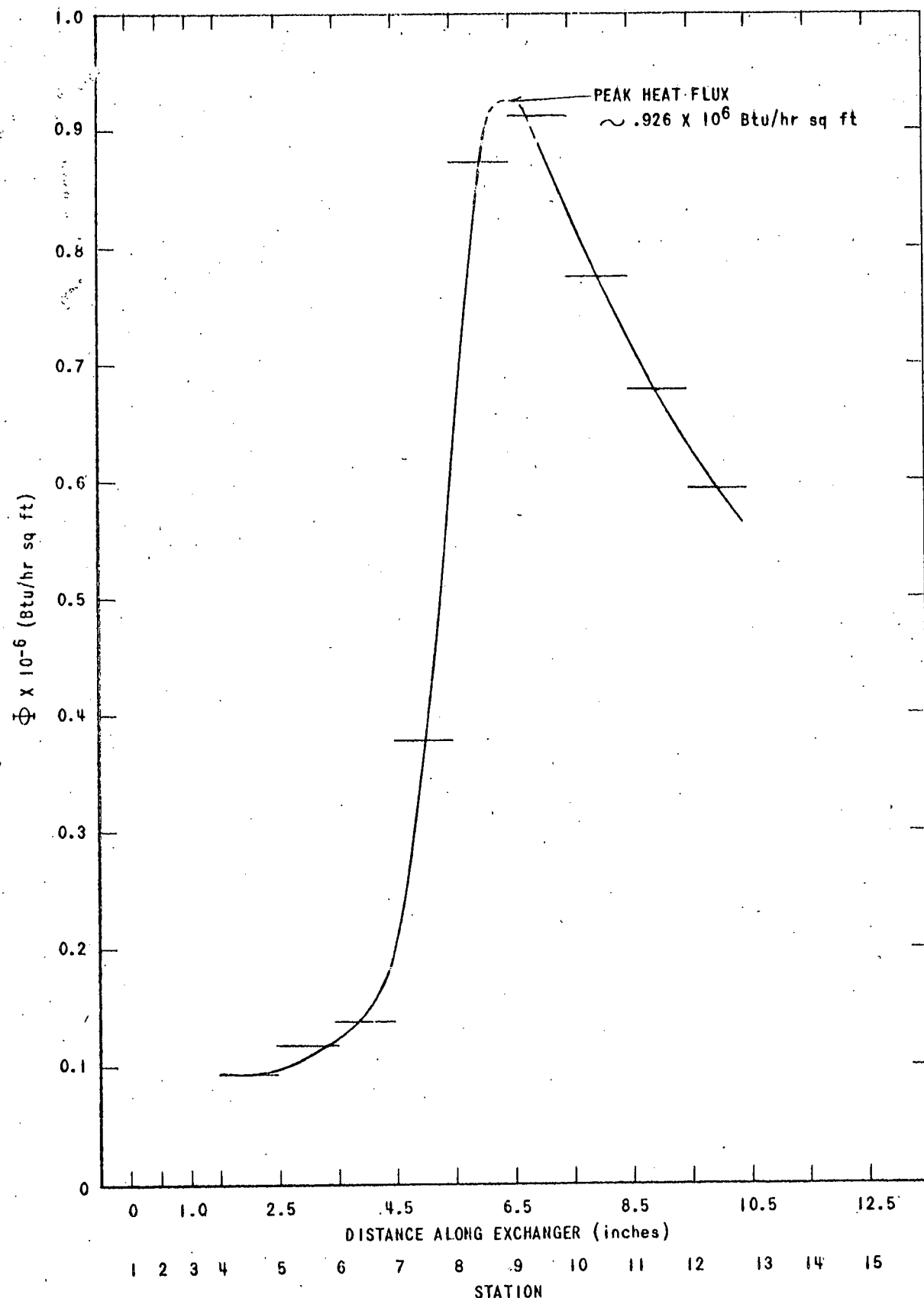


Fig. 5 - Heat Flux vs Distance Along Exchanger - Run 6-2

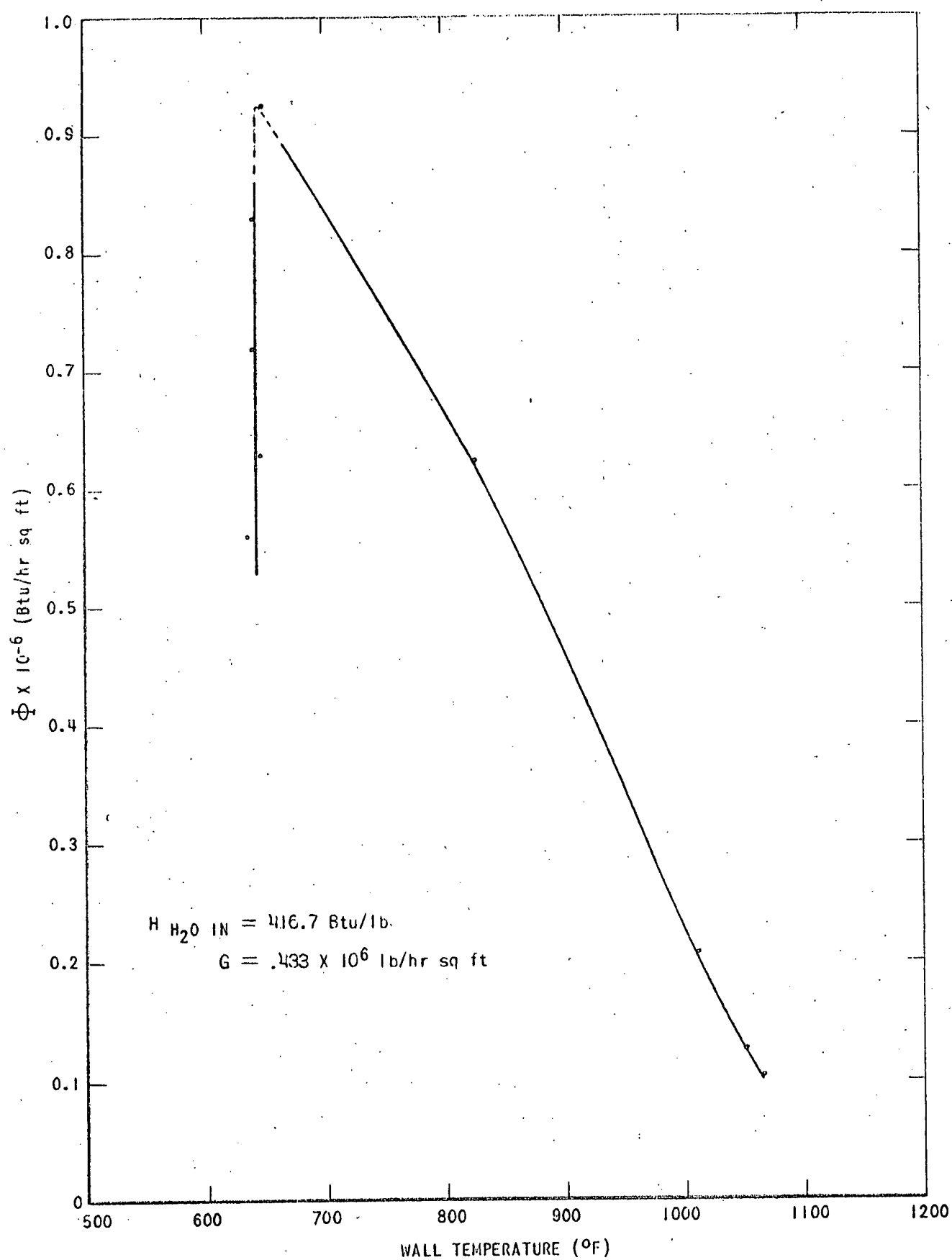


Fig. 6 - Heat Flux vs Wall Temperature - Run 6-2

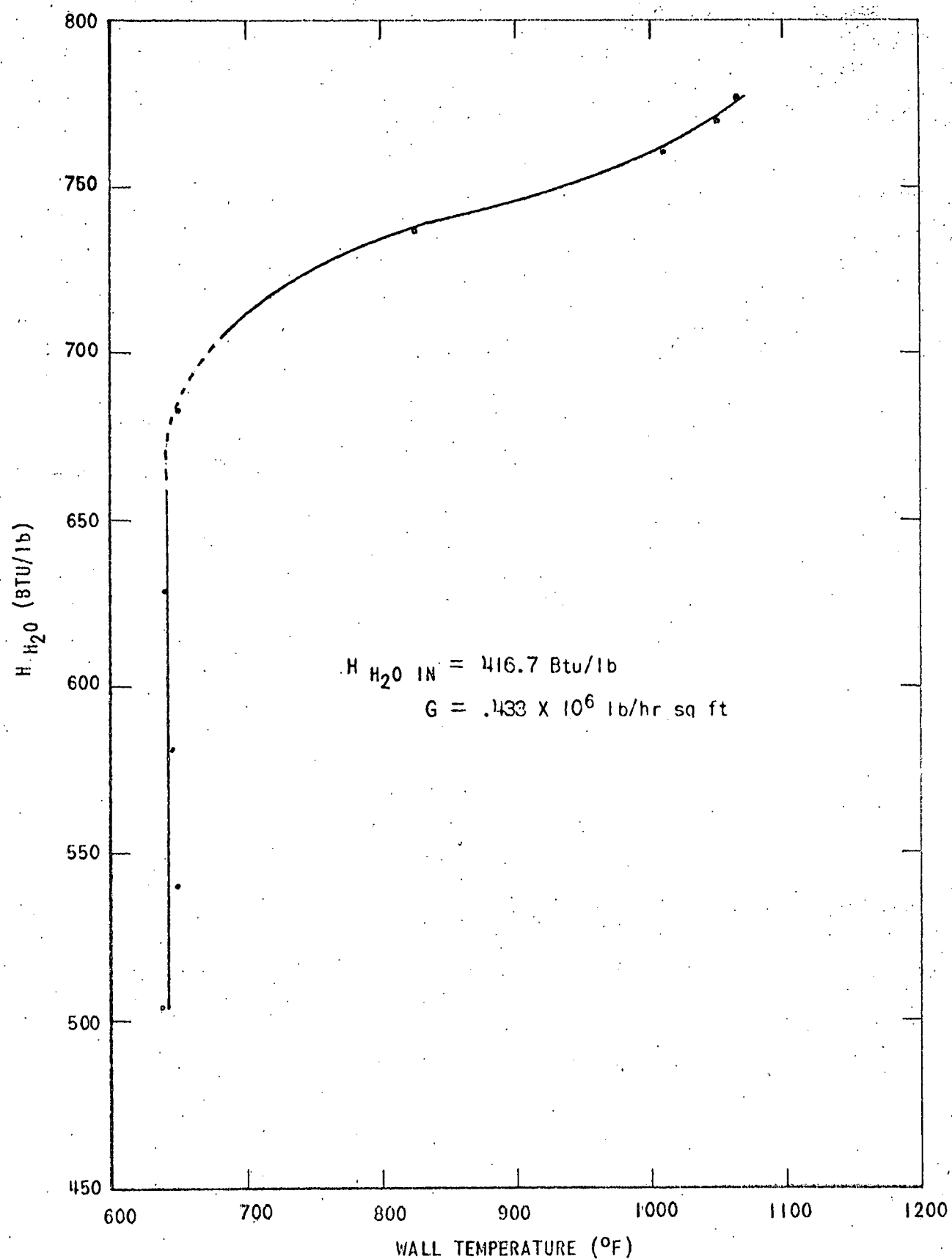


Fig. 7. - Enthalpy vs Wall Temperature - Run 6-2

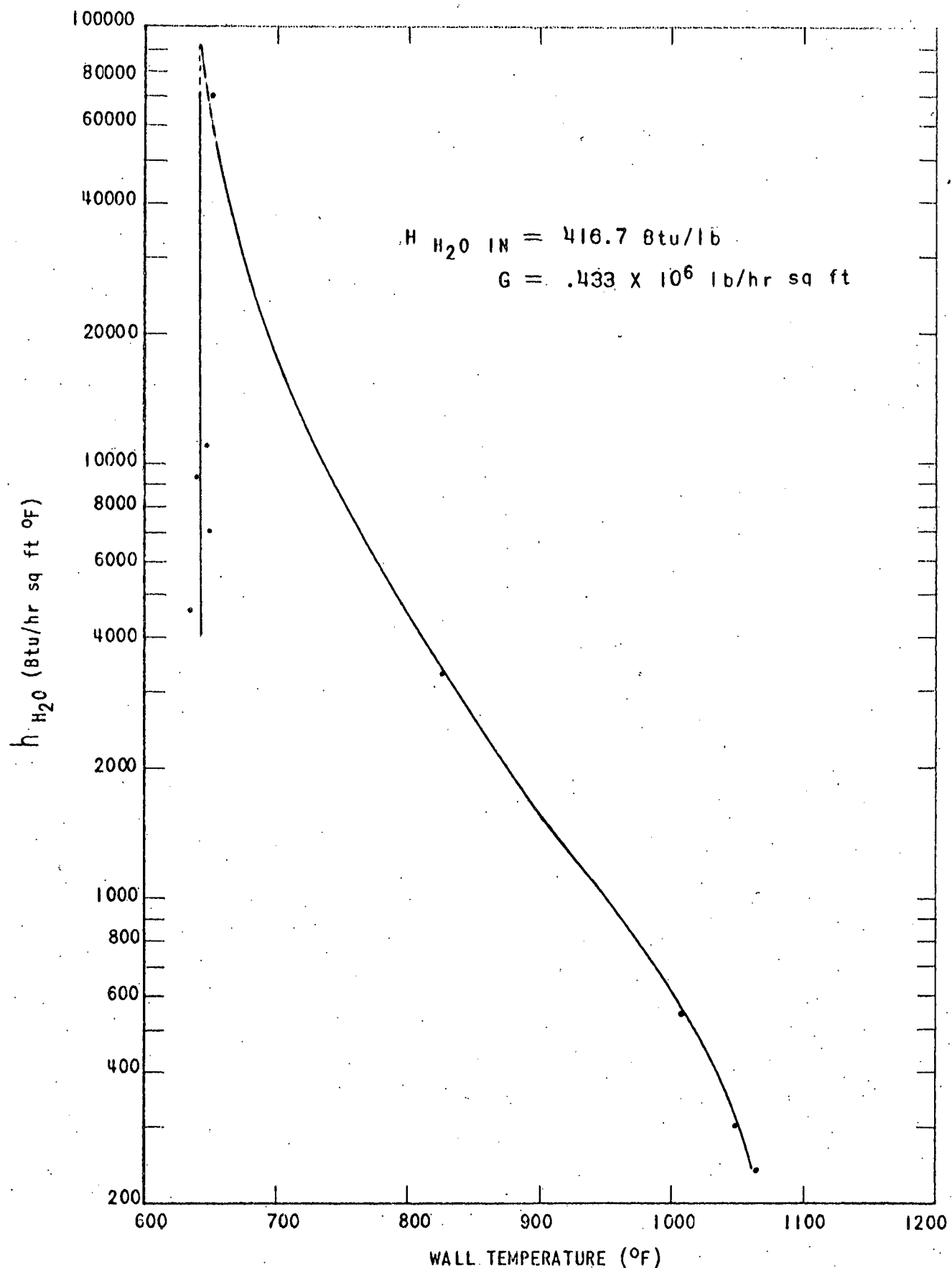


Fig. 8 - Water Coefficient vs Wall Temperature - Run 6-2

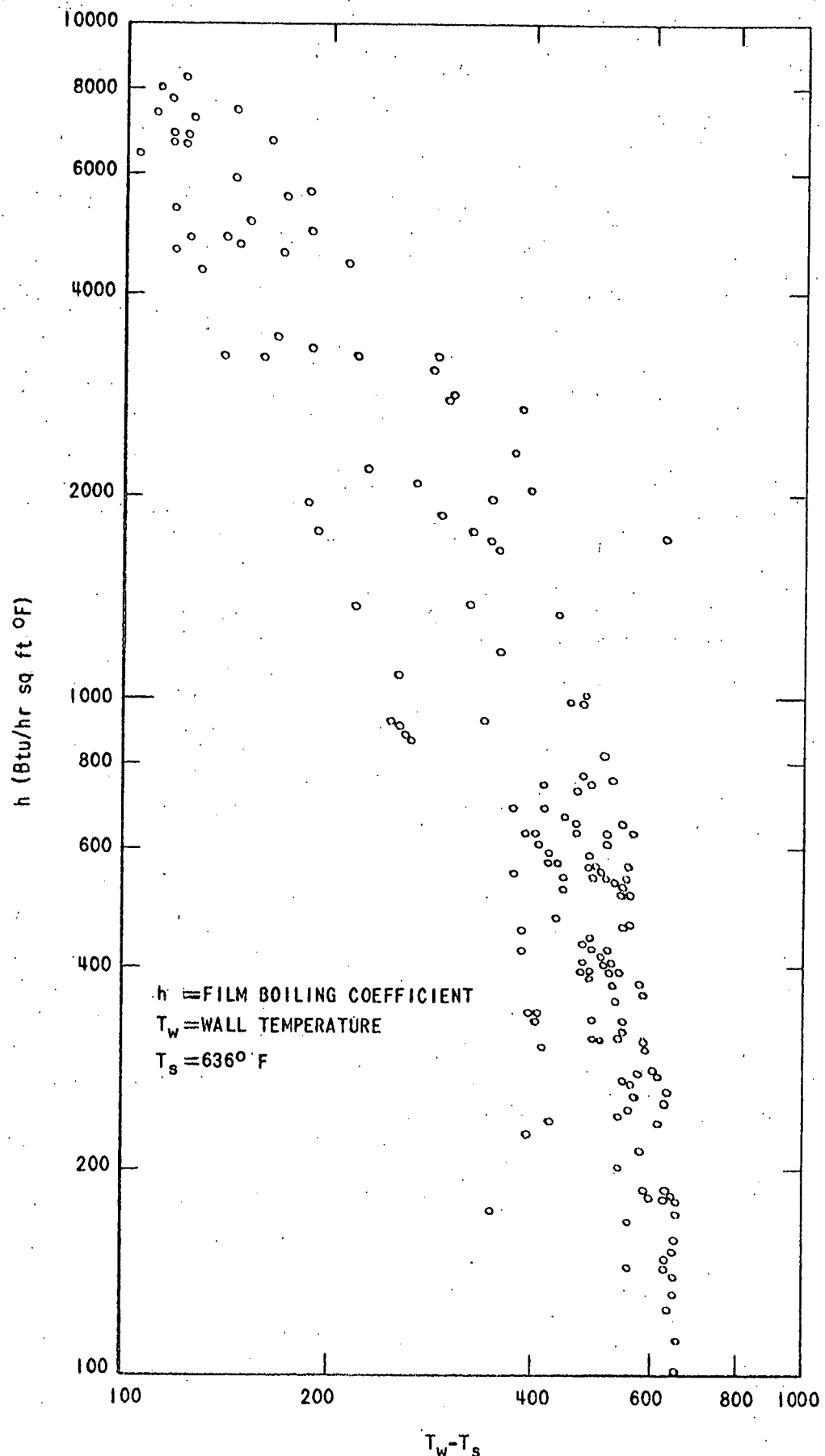


Fig. 9 - Partial Film Boiling Coefficients vs  $T_w - T_s$

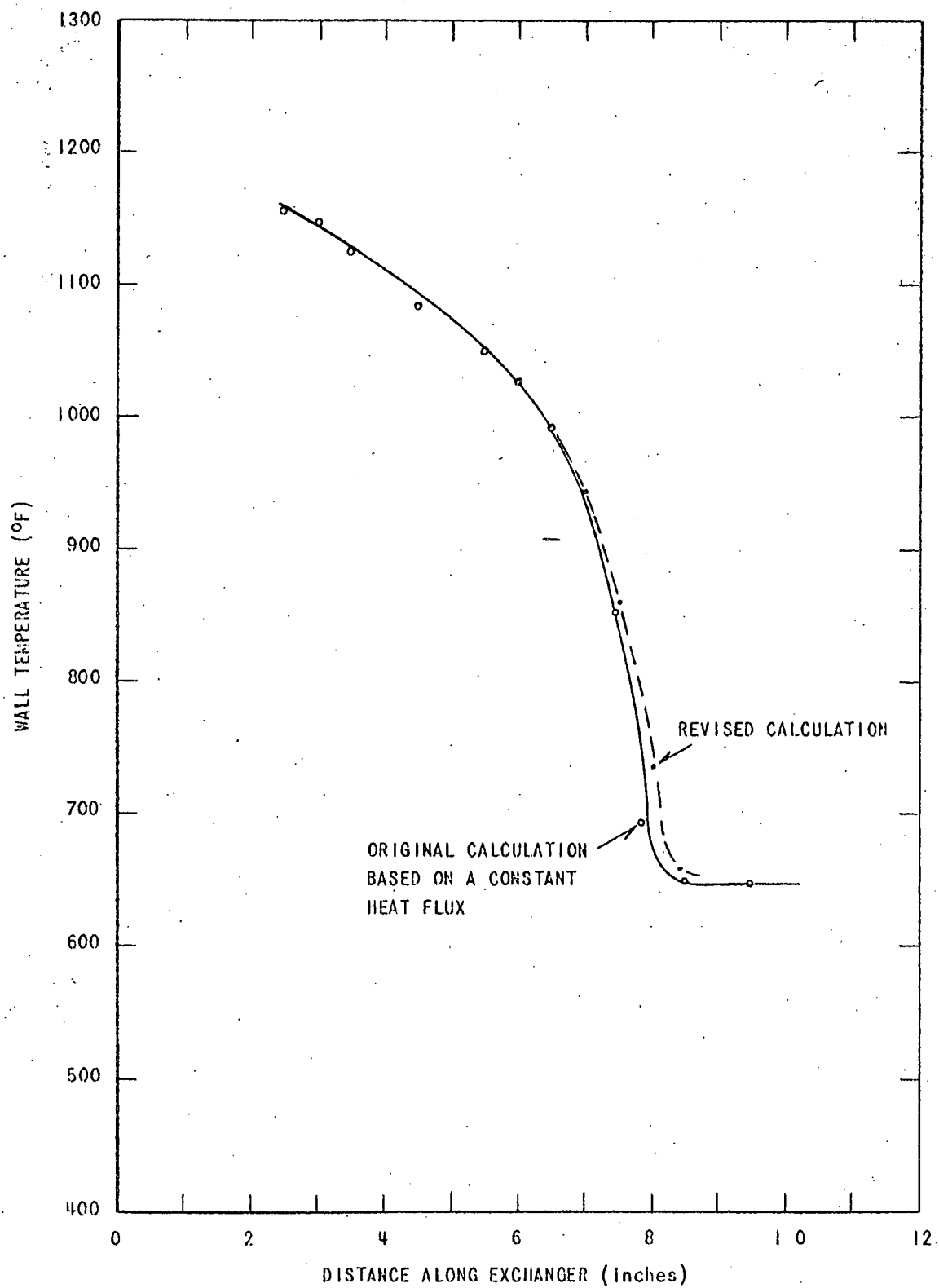


Fig. 10 - Results of Variable Heat Flux on NaK Conductance  
Run 11-2

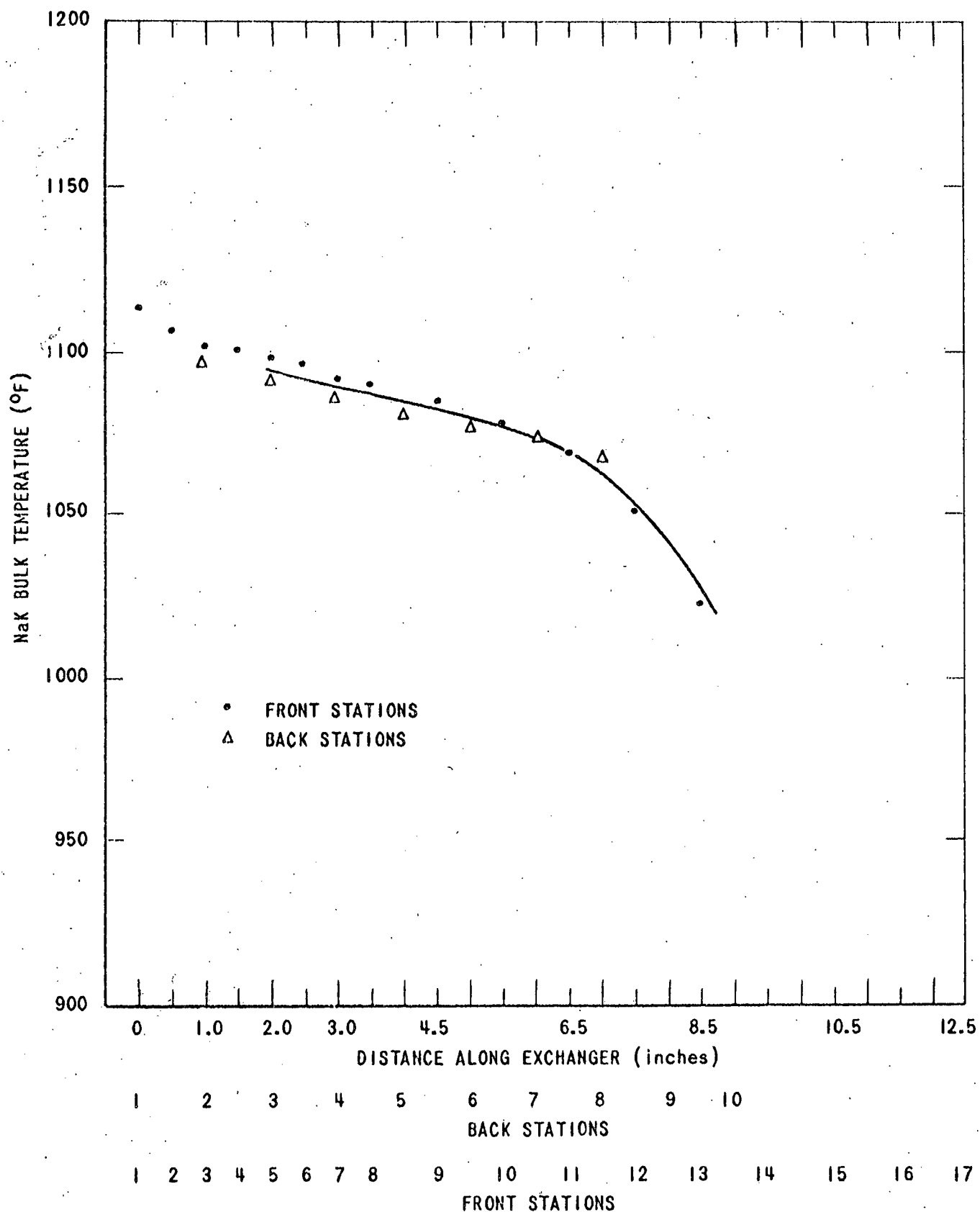


Fig. 11 - NaK Bulk Temperature vs Distance Along Exchanger  
Run 15-2

Table 1 - Heat Transfer Coefficients of Water Inside Tube  
0.152 ID x 12-1/2 in. In Length

Run No.	Station	Water Inlet Enthalpy (Btu/lb)	Mass Flow Rate (lb/hr-ft <sup>2</sup> x 10 <sup>6</sup> )	L/D*	Water Enthalpy (Btu/lb)	Tube Wall Temp. (T <sub>w</sub> °F)	Local Heat Flux (Btu/hr-ft <sup>2</sup> x 10 <sup>6</sup> )	Water Side Heat Transfer Coefficient (Btu/hr-ft <sup>2</sup> -°F)	T <sub>w</sub> -T <sub>H2O</sub> (°F)
1-2	6	377.0	0.428	59.2	745.0	1192	0.08	144	556
	7				52.6	739.6	1175	0.11	204
	8				46.0	730.6	1127	0.21	427
	9				39.5	711.3	960	0.575	1,770
	10				32.9	643.8	645	1.131	43,600
1-1	5	380.2	0.421	59.2	752.3				
	6				59.2	743.2	1069	0.206	476
	7				52.6	725.8	957	0.44	1,370
	8				46.0	672.8	693	0.935	16,400
	9				39.5	607.8	639	0.875	19,900
	10				32.9	548.4	647	0.714	7,440
	11				26.3	506.2	640	0.604	4,870
	12				19.7	471.5	645	0.513	3,220
	5	378	0.444	59.2	740.0				
	6				59.2	735.6	1284	0.073	113
	7				52.6	731.2	1276	0.080	125
	8				46.0	728.0	1266	0.094	149
	9				39.5	721.9	1250	0.115	187
	10				32.9	714.1	1217	0.18	310
	11				26.3	697.6	1092	0.45	988
	12					660.1			
2-1	5	378.0	0.555	59.2	697.1				
	6				59.2	690.1	1097	0.30	651
	7				52.6	667.0	850	0.815	3,760
	8				46.0	616.8	647	1.115	24,850
	9				39.5	568.0	640	1.08	14,600
	10				32.9	525.4	634	0.816	8,000
	11				26.3	489.9	639	0.682	4,970
2-2	4	378.0	0.548	59.2	679.9				
	5				65.7	666.3	908	0.56	2,030
	6				59.2	631.0	734	0.84	6,830
	7				52.6	588.2	648	0.880	13,300
	8				46.0	549.4	646	0.740	7,880
	9				39.5	516.7	643	0.625	5,300
2-3	5	377.0	0.557	59.2	701.7				
	6				59.2	696.7	1249	0.105	171
	7				52.6	690.7	1213	0.16	277
	8				46.0	677.9	934	0.825	2,760
	9				39.5	626.7	636	1.25	45,300
	10				32.9	569.5	647	1.097	13,700
	11				26.3	521.8	643	0.915	804
3-1	4	380.2	0.705	59.2	719.6				
	5				65.7	715.8	1171	0.13	243
	6				59.2	709.2	1104	0.29	618
	7				52.6	681.5	821	0.94	5,070
	8				46.0	639.9	677	1.165	19,400
	9				39.5	592.2	641	1.12	19,700
	10				32.9	552.1	640	1.04	12,200
	11				26.3	516.8	741	0.917	7,800
	12				19.7	484.3	637	0.844	5,880
	5								
	6								
	7								

\* See Fig. 2, page 17 for method for determining L.

Table 1 - Heat Transfer Coefficients of Water Inside Tube  
0.152 ID x 12-1/2 in. In Length - continued

Run No.	Station	Water Inlet		L/D*	Water		Tube Wall		Water Side Heat		T <sub>w</sub> -T <sub>H2O</sub> (°F)
		Enthalpy (Btu/lb)	Mass Flow Rate (lb/hr-ft <sup>2</sup> x 10 <sup>6</sup> )		Enthalpy (Btu/lb)	(T <sub>w</sub> ) Temp. (°F)	Local Heat Flux (Btu/hr-ft <sup>2</sup> x 10 <sup>6</sup> )	Transfer Coefficient (Btu/hr-ft <sup>2</sup> , °F)			
4-1	4	378.0	0.732		651.7	-	-	-	778	-	-
	5	-	-		657.0	1098	0.37	-	-	476	476
	6	-	-		620.6	815	0.94	4,450	-	211	-
	7	-	-		581.0	640	1.15	18,000	-	64	-
	8	-	-		543.0	642	0.965	10,020	-	96	-
	9	-	-		510.7	640	0.820	6,830	-	120	-
	10	-	-		483.2	638	0.698	4,900	-	142	-
	11	-	-		460.1	639	0.582	3,550	-	164	-
	4-2		378.0		662.0	-	-	-	-	-	-
	5	-	-		660.0	1270	0.09	140	-	641	-
	6	-	-		654.1	1178	0.31	561	-	552	-
	7	-	-		632.0	917	0.86	2,820	-	305	-
	8	-	-		589.0	645	1.3	20,700	-	63	-
	9	-	-		544.3	638	1.09	12,100	-	90	-
	10	-	-		507.7	639	0.915	7,50	-	122	-
	11	-	-		477.1	638	0.78	5,300	-	147	-
5-1	5	374.0	0.977		645.8	-	-	-	-	-	-
	6	-	-		633.0	1005	0.89	227	-	392	-
	7	-	-		596.7	692	1.465	14,600	-	105	-
	8	-	-		556.4	637	1.392	17,400	-	80	-
	9	-	-		521.3	-	-	-	-	-	-
6-1	5	416.7	0.433		65.7	690.1	665	0.650	22,300	-	29
	6	-	-		59.2	649.9	642	0.620	34,400	-	18
	7	-	-		52.6	614.6	645	0.54	12,000	-	45
	8	-	-		46.0	584.1	647	0.475	6,980	-	68
	9	-	-		39.5	557.2	644	0.425	4,940	-	86
	10	-	-		32.9	532.8	643	0.380	3,620	-	105
	11	-	-		26.3	510.9	642	0.338	2,810	-	120
	12	-	-		19.7	491.3	643	0.30	2,140	-	140
	13	-	-		13.2	474.3	643	0.266	1,720	-	155
	6-2		411.1		0.435 x 10 <sup>6</sup>	783.1	-	-	-	-	-
	5	-	-		65.7	777.0	1064	0.102	238	-	428
	6	-	-		59.2	769.7	1049	0.125	303	-	413
	7	-	-		52.6	761.2	1010	0.207	554	-	374
	8	-	-		46.0	738.1	824	0.625	3,320	-	188
	9	-	-		39.5	684.7	649	0.925	71,100	-	13
	10	-	-		32.9	629.0	641	0.83	26,800	-	31
	11	-	-		26.3	581.7	646	0.72	10,400	-	69
	12	-	-		19.7	540.1	648	0.63	6,120	-	103
	13	-	-		13.2	504.1	636	0.56	4,580	-	122
6-3	4	416.7	0.433		72.3	809.6	1228	0.109	184	-	592
	5	-	-		65.7	802.9	1224	0.11	187	-	588
	6	-	-		59.2	796.2	1215	0.124	215	-	579
	7	-	-		52.6	786.1	1201	0.146	258	-	565
	8	-	-		46.0	776.0	1184	0.176	322	-	548
	9	-	-		39.5	764.2	1162	0.213	405	-	526
	10	-	-		32.9	749.1	1105	0.344	734	-	469
	11	-	-		26.3	720.5	985	0.610	1,750	-	349
	12	-	-		19.7	672.2	808	0.965	5,600	-	172
	13	-	-		13.2	605.7	-	-	-	-	-
	6-4		415.6		0.421	818.6	-	-	-	-	-
	5	-	-		65.7	811.3	1294	0.120	182	-	658
	6	-	-		59.2	804.0	1292	0.110	168	-	656
	7	-	-		52.6	796.7	1288	0.103	158	-	652
	8	-	-		46.0	789.4	1276	0.118	184	-	640
	9	-	-		39.5	782.0	1254	0.163	263	-	618
	10	-	-		32.9	767.3	1198	0.26	464	-	560
	11	-	-		26.3	750.2	1112	0.47	988	-	476
	12	-	-		19.7	708.6	923	0.865	3,010	-	281
	13	-	-		-	642.6	-	-	-	-	-
	14	-	-		-	575.3	-	-	-	-	-

\* See Fig. 2, page 17 for method for determining L.

Table 1 - Heat Transfer Coefficients of Water Inside Tube  
0.152 ID x 12-1/2 in. in Length - continued

Run No.	Station	Water Inlet Enthalpy (Btu/lb)	Mass Flow Rate (lb/hr-ft <sup>2</sup> x 10 <sup>6</sup> )	L/D*	Water Enthalpy (Btu/lb)	Tube Wall Temp. (°F)	Local Heat Flux (Btu/hr-ft <sup>2</sup> x 10 <sup>6</sup> )	Water Side Heat Transfer Coefficient (Btu/hr-ft <sup>2</sup> -°F)	T <sub>w</sub> -T <sub>H2O</sub> (°F)
7-1	5				59.2	711.4	1277	0.97	151
	6	416.7	0.54		52.6	704.0	1275	0.91	142
	7				46.0	697.6	1262	0.109	639
	8				39.5	690.1	1242	0.142	626
	9				32.9	678.0	1205	0.206	606
	10				26.3	656.5	1142	0.318	569
	11				19.7	611.7	947	0.69	514
	12				13.2	555.7	719	1,980	349
	13							6,700	163
7-2	5	417.8	0.555		716.8				
	6				59.2	702.8	928	0.55	1,880
	7				52.6	660.8	704	0.92	12,400
	8				46.0	616.8	652	0.875	17,500
	9				39.5	577.6	637	0.76	12,100
	10				32.9	544.0	639	0.652	7,160
	11				26.3	515.3	640	0.55	4,740
	12				19.7	491.5	647	0.45	116
								3,130	144
8-1	5	413.4	0.641 x 10 <sup>6</sup>		65.7	662.1	1285	0.066	101
	6				59.2	658.9	1275	0.085	131
	7				52.6	655.0	1260	0.115	182
	8				46.5	649.5	1237	0.156	254
	9				39.5	642.4	1206	0.215	587
	10				32.9	632.2	1162	0.300	545
	11				26.3	617.3	1074	0.475	550
	12					566.4		1,000	472
8-2	5	415.6	0.65						
	6				59.2	699.4	1195	0.138	247
	7				52.6	693.5	1176	0.17	315
	8				46.5	685.1	1128	0.27	549
	9				39.5	670.0	983	0.60	492
	10				32.9	615.6	636	1.260	348
	11				26.3	567.0	637	1.11	36,000
	12							15,600	35
									71
9-1	5	415.6	0.967 x 10 <sup>6</sup>			669.5			
	6				59.2	662.1	1178	0.355	649
	7				52.6	648.2	1009	0.8	2,070
	8				46.0	611.5	679	1.41	386
	9				39.5	573.6	639	1.318	17,400
	10				32.9	540.1	638	1.16	19,100
	11				26.3	510.4	636	1.025	12,300
	12				19.7	484.5	637	0.906	8,800
								6,470	94
									116
									140
10-1	6				65.7	819.3			
	7	486.3	0.424 x 10 <sup>6</sup>		62.5	811.3	855	0.289	1,320
	8				59.2	801.8	828	0.345	1,795
	9				52.6	774.7	735	0.523	192
	10				46.0	733.4	638	0.687	5,270
	11				39.5	693.5	642	0.613	343,500
	12				26.3	656.8	639	0.558	102,000
	13							46,500	6
									12
10-2	6	487.4	0.416		65.7	895.1	1140	0.159	315
	7				62.5	885.0	1137	0.159	504
	8				59.2	874.9	1134	0.159	501
	9				52.6	864.8	1126	0.165	498
	10				46.0	853.0	1108	0.193	490
	11				39.5	841.2	1085	0.235	449
	12				26.3	824.4	1055	0.290	472
	13							692	419

\* See Fig. 2, page 17 for method for determining L.

Table 1 - Heat Transfer Coefficients of Water Inside Tube  
0.152 ID x 12-1/2 in. In Length - continued

Run No.	Station	Water Inlet Enthalpy (Btu/lb)	Mass Flow Rate (lb/hr-ft <sup>2</sup> x 10 <sup>6</sup> )	L/D*	Water Enthalpy (Btu/lb)	Tube Wall Temp. (T <sub>w</sub> ) (°F)	Local Heat Flux (Btu/hr-ft <sup>2</sup> x 10 <sup>6</sup> )	Water Side Heat Transfer Coefficient (Btu/hr-ft <sup>2</sup> -°F)	T <sub>w</sub> -T <sub>H2O</sub> (°F)
10-3	6	486.3	0.436	65.7	825.3	1183	0.176	321	547
	7			62.5	820.0	1180	0.176	329	544
	8			59.2	814.7	1177	0.176	326	541
	9			52.6	804.1	1166	0.189	357	530
	10			46.0	791.7	1149	0.217	424	513
	11			39.5	777.5	1120	0.274	566	484
	12			26.3	758.0	1032	0.480	1,210	396
	13			-	-	-	-	-	-
11-1	6	485.0	0.634	65.7	642.9	1011	0.135	345	392
	7			62.5	640.1	1002	0.175	455	385
	8			59.2	635.4	959	0.273	790	345
	9			52.6	617.6	772	0.69	4,060	170
	10			46.0	581.1	642	0.906	13,700	66
	11			39.5	547.5	648	0.79	8,580	98
11-2	6	485.1	0.632	65.7	767.2	1123	0.19	389	487
	7			62.5	763.1	1119	0.195	395	483
	8			59.2	758.9	1110	0.205	432	474
	9			52.6	748.6	1084	0.245	546	448
	10			46.0	735.6	1050	0.308	743	414
	11			39.5	734.1	994	0.418	1,170	358
	12			32.9	712.4	854	0.715	3,270	218
	13			26.3	668.8	648	1.095	78,200	14
	14			49.2	624.3	648	0.98	23,900	41
11-3	5	485.1	0.648	69.1	784.6	1243	0.168	277	607
	6			65.7	781.2	1240	0.168	279	604
	7			62.5	777.8	1237	0.168	280	601
	8			59.2	774.4	1234	0.168	281	598
	9			52.6	767.6	1223	0.180	307	587
	10			46.0	759.6	1207	0.205	359	571
	11			39.5	750.8	1183	0.25	456	547
	12			32.9	739.1	1151	0.31	603	515
	13			26.3	-	-	-	-	-
12-1	6	487.4	1 x 10 <sup>6</sup>	65.7	705.0	1187	0.149	270	551
	7			62.5	702.9	1184	0.149	272	548
	8			59.2	700.8	1163	0.20	379	527
	9			52.6	694.3	1122	0.36	741	486
	10			46.0	682.5	988	0.584	1,660	352
	11			39.5	662.2	817	0.931	5,000	186
	12			26.3	633.4	638	1.235	49,400	25
	13			-	-	-	-	-	-
13-1	5	486.3	1.45	69.1	673.6	1163	0.4	760	527
	6			65.7	669.8	1145	0.425	833	510
	7			62.5	665.6	1065	0.58	1,340	432
	8			59.2	657.2	916	0.93	3,230	288
	9			52.6	636.3	719	1.275	12,300	104
	10			46.0	611.3	643	1.288	28,500	45
	11			39.5	589.1	646	1.146	17,900	64
	12			32.9	569.1	635	1.05	15,400	68
14-1	6	614.4	0.444	65.7	907.6	900	0.23	872	264
	7			62.5	895.5	898	0.23	878	262
	8			59.2	883.4	895	0.23	890	259
	9			52.6	871.3	890	0.23	906	254
	10			46.0	859.2	883	0.23	930	247
	11			39.5	847.1	821	0.362	1,960	185
	12			32.9	821.4	739	0.523	5,080	103
	13			-	-	-	-	-	-

\* See Fig. 2, page 17 for method for determining L.

Table 1 - Heat Transfer Coefficients of Water Inside Tube  
 0.152 ID x 12-1/2 in. In Length - continued

Run No.	Station	Water Inlet Enthalpy (Btu/lb)	Mass Flow Rate (lb/hr-ft <sup>2</sup> x 10 <sup>6</sup> )	L/D*	Water Enthalpy (Btu/lb)	Tube Wall (T <sub>w</sub> ) Temp. (°F)	Loval Heat Flux (Btu/hr-ft <sup>2</sup> x 10 <sup>6</sup> )	Water Side Heat Transfer Coefficient (Btu/hr-ft <sup>2</sup> -°F)	T <sub>w</sub> -T <sub>H2O</sub> (°F)
14-2	5	613.0	0.444	69.1	968.0	1069	0.247	572	433
	6			65.7	960.6	1064	0.247	578	428
	7			62.5	953.2	1059	0.247	587	423
	8			59.2	945.8	1055	0.249	590	419
	9			52.6	931.0	1046	0.247	603	410
	10			46.0	912.9	1037	0.247	617	401
	11			39.5	898.1	1027	0.247	633	391
	12			32.9	880.0	1012	0.262	697	376
	13			-	-	-	-	-	-
	-----								
14-3	6	614.4	0.446	65.7	973.2	1188	0.283	513	552
	7			62.5	963.8	1183	0.283	518	547
	8			59.2	954.4	1177	0.283	524	541
	9			52.6	945.0	1166	0.283	534	530
	10			46.0	935.6	1155	0.283	546	519
	11			39.5	926.2	1145	0.283	557	509
	12			32.9	916.8	1135	0.283	568	499
	13			26.3	907.4	1125	0.283	580	489
	-----								
15-1	4	614.4	0.606 x 10 <sup>6</sup>	72.5	890.6	1167	0.21	396	531
	5			69.1	886.0	1163	0.21	398	527
	6			65.7	881.4	1159	0.21	402	523
	7			62.5	876.8	1155	0.21	404	519
	8			59.2	892.7	1151	0.21	407	515
	9			52.6	861.9	1141	0.21	416	505
	10			46.0	852.7	1133	0.21	423	497
	11			39.5	843.5	1123	0.217	446	487
	12			32.9	833.2	1084	0.296	661	448
	13			26.3	816	1007	0.458	1,232	371
	14			-	-	-	-	-	-
	-----								
15-2	6			65.7	870.4	1042	0.137	337	406
	7			62.5	864.3	1039	0.137	340	403
	8			59.2	858.2	1037	0.137	342	401
	9			52.6	852.1	1032	0.137	346	396
	10			46.0	846.0	1017	0.162	426	381
	11			39.5	836.3	956	0.30	937	320
	12			32.9	815.8	862	0.497	2,200	226
	13			26.3	789.1	752	0.71	6,070	117
	14			-	-	-	-	-	-

\* See Fig. 2, page 17 for method for determining L.

Table 2 - Comparison of MSAR Data and WAPD Burnout Flux

Run	$B.O. \times 10^{-6}$ (Btu/hr-ft <sup>2</sup> )	Local Enthalpy (Btu/lb)	L/D	WAPD B.O. $\times 10^{-6}$ Prediction	% Deviation from MSAR B.O.
1-1	0.95	620	44.4	0.97	2.1
1-2	1.13	643	32.9	0.88	-22.1
2-1	1.12	620	47.4	0.96	-14.3
2-2	0.91	588	55.9	1.10	20.8
2-3	1.25	630	39.4	0.94	-24.8
3-1	1.18	610	44.7	1.01	-14.4
4-1	1.17	582	53.9	1.13	-3.4
4-2	1.30	590	46.0	1.10	-15.4
5-1	1.52	560	50.6	1.24	-18.4
6-1	0.935	674	39.4	0.81	-12.9
7-1	1.18	553	11.1	1.28	8.5
7-2	0.94	610	50.6	1.00	6.4
8-2	1.33	616	35.5	1.05	-21.0
9-1	1.41	585	44.7	1.11	-21.2
9-2	1.20	605	61.2	1.02	-15.0
10-1	0.69	740	47.4	0.62	-10.0
11-1	0.91	582	48.0	1.13	24.1
11-2	1.10	670	26.3	0.83	-24.5
12-1	1.23	633	32.8	0.94	-23.5
13-1	1.36	611	49.5	1.05	-22.8

## APPENDIX II

DETERMINATION OF THE LOCAL NUSSELT NUMBER  
FOR FLOW THROUGH AN ANNULUS WITH HEAT TRANSFER  
FROM ONE SIDE

## NOMENCLATURE FOR APPENDIX 11\*

English Letter Symbols

- a - constant in Table 1, dimensionless, and constant\*\* in eq. (13),  $^{\circ}\text{F}$
- b - constant in eq. (13),  $^{\circ}\text{F}$
- c - specific heat, Btu/(lb  $^{\circ}\text{F}$ )
- C - constants in Table 1, dimensionless
- $C_n$  - constants in eq. (3), dimensionless
- D - flow tube diameter, ft
- g - functions of  $x^+$  and  $r^+$  defined by eq. (18), dimensionless
- $G_n$  - constants defined by eq. (4), dimensionless
- $H^2$  - functions of  $r_m^2$  defined by eq. (20), dimensionless
- L - dummy integration variable varying from 0 to  $x^+$ , dimensionless
- q - heat flux at surface of tube, Btu/(hr. sq ft)
- r - radial distance from center of flow tube, ft
- $r_o$  - flow tube radius, ft
- $r^+$  -  $r/r_o$ , dimensionless
- t - Temperature,  $^{\circ}\text{F}$
- $t_o$  - Coolant temperature at tube entrance,  $^{\circ}\text{F}$
- $t_w$  - Coolant tube wall surface temperature,  $^{\circ}\text{F}$ .

---

\* Taken directly from; Kays, W. M., and Nicoll, W. B., The Influence of Non-Uniform Heat Flux on the Convection Conductances in a Nuclear Reactor, Technical Report 33 (Contract Nonr 225(23) NR-065-104) Stanford University, November 1, 1957.

\*\* Tables and equations in the nomenclature refer to W. M. Kays' report.

## Nomenclature for Appendix 11 - continued

$x$  - axial distance from tube entrance, ft

$x^+$  -  $(s/r_o)(N_R N_{Pr})$ , dimensionless

Greek Letter Symbols

$\beta$  - dimensionless parameter defined by eq. (26)

$\sqrt{m}$  - eigenvalues for constant heat flux problem,  
dimensionless

$\lambda_n^2$  - eigenvalues for constant surface temperature  
problem, dimensionless

Non-Dimensionless Groupings

$Nu$  - Nusselt number  $hD/k$ ,  $2 hr_o/k$

$N_{Pr}$  - Prandtl number,  $\mu c_p/k$ ,  $\mu c/k$

$N_R$  - Reynolds number,  $DV_p/\mu$ ,  $2r_o V_p/\mu$

## APPENDIX 11

The following analysis suggested by Kays<sup>10</sup> was used to determine the effect of variable axial heat flux on the local Nusselt number. At the present there is no data available to predict the local Nusselt number for flow through an annulus with heat transfer from one side. However, there are data for such an analysis for flow in a circular tube. Therefore, the following method<sup>9, 10</sup> is carried out assuming the annulus is a tube.

Method

$$(t_w - t_o) = \frac{r_o}{k} \int_0^{x^+} g(x^+ - L, 1) q(L) dL \quad \text{eq. 7}$$

Since  $q(L)$  is negative in this case

$$t_w = t_o - \frac{r_o}{k} \int_0^{x^+} g(x^+ - L, 1) q(L) dL \quad \text{eq. 8}$$

By an Energy Balance

$$t = t_o - 4 \frac{r_o}{k} \int_0^{x^+} q(L) dL \quad \text{eq. 9}$$

By definition

$$Nu = \frac{hD}{k} = \frac{2q r_o}{(t - t_w)k} \quad \text{eq. 10}$$

on Sub.

$$Nu = \frac{2q r_o}{\left[ t_o - \frac{4r_o}{k} \int_0^{x^+} q(L) dL - t_o + \frac{r_o}{k} \int_0^{x^+} g(x^+ - L, 1) q(L) dL \right]^k}$$

then

$$Nu = \frac{2q}{\int_0^{x^+} g(x^+ - L, 1) q(L) dL - 4 \int_0^{x^+} q(L) dL} \quad \text{eq. 11}$$

For the purpose of this analysis a typical test run (11-2) was chosen for study. The Peclet number for this run is approximately 100, therefore, knowing the Peclet number the following table of eigenvalues was chosen from Kays' and Nicoll's report<sup>9</sup>:

Table of Eigenvalues and Constants  
for  $Pr = 0.01$ ,  $N_R = 10,000$

<u><math>\lambda_n^2</math></u>	<u><math>G_n</math></u>	<u><math>\gamma_m^2</math></u>	<u><math>-H^*(-\gamma_m^2)</math></u>
10.2	0.964	-	-
56.3	0.810	30.2	$7.34 \times 10^{-3}$
142	0.760	98.5	$2.04 \times 10^{-3}$
266	0.728	206	$0.935 \times 10^{-3}$
429	0.704	353	$0.528 \times 10^{-3}$
630	0.685	539	$0.334 \times 10^{-3}$

$$Nu_t = 5.10 \frac{Nu}{Nu_H} = 6.46$$

### Procedure

Using the Eigenvalues and constants, the table of heat fluxes, Table 3, was constructed for run (11-2) using  $1.95 \times 10^5$  Btu/hr sq ft at the  $x^+ = 0$  where  $x = 1^{\text{st}}$  position, and  $10.62 \times 10^5$  Btu/hr sq ft as the heat flux at  $x^+ = 0.540$ ,  $x = 9^{\text{th}}$  position.

Table 3 - Heat Fluxes for Run 11-2

<u>x</u> Inches of Annulus	<u>x<sup>+</sup></u>	Heat Flux <u>q x 10<sup>-5</sup></u> Btu/hr sq ft
1	0	1.9
1.5	0.0338	1.9
2.0	0.0675	1.9
2.5	0.1015	1.9
3.0	0.135	1.9
3.5	0.169	2.0
4.0	0.203	2.2
4.5	0.236	2.4
5.0	0.270	2.7
5.5	0.304	3.1
6.0	0.338	3.5
6.5	0.372	4.2
7.0	0.405	5.3
7.5	0.438	7.2
8.0	0.473	10.1
8.5	0.507	11.0
9.0	0.540	10.62

With the aid of the table the following function can now be evaluated:

$$g(x^+ - L, 1) = 4 + \sum_m \frac{e^{-\gamma_m^2(x^+ - L)}}{\gamma_m^2(-H^1(\gamma_m^2))} \quad \text{eq. 12}$$

on sub. in equation 11.

$$Nu = \frac{2q}{\int_0^{x^+} (L) \left[ \sum_m \frac{e^{-\gamma_m^2(x^+ - L)}}{\gamma_m^2(-H^1(\gamma_m^2))} \right] dL} \quad \text{eq. 13}$$

First evaluating the integrals at  $x^+ = 0.338$

Table 4 - Evaluation of Integral for Run 11-2

Consider  $x = 0.338$ 

$L$	$x^+ - L$	$q(L)$	$\gamma_m^2(x-L)$	$\gamma_m^2(x-L)$	$\gamma_m^2(x-L)\gamma_m^2(-H)$	$q(L) \times 10^{-5}$
0	0.338	1.9	10.2		0.0	0.0
0.0338	0.304	1.9	9.18	9600	0.0005	0.00095
0.0675	0.270	1.9	8.15	3500	0.0013	0.00247
0.1015	0.236	1.9	7.13	1250	0.0036	0.00684
0.1350	0.203	1.9	6.13	460	0.0098	0.0180
0.1690	0.169	2.0	5.1	165	0.0273	0.0540
0.203	0.135	2.2	4.07	59	0.0764	0.1680
0.236	0.102	2.4	3.08	21.7	0.207	0.496
0.270	0.068	2.7	6.7	810	0.005	1.57
			2.05	7.8	0.576	
					0.581	
0.304	0.034	3.1	3.35	28.5	1.62	5.50
			1.025	2.78	0.158	
					1.778	
0.338	0	3.5	1			

This gives the integral up to  $L = 0.304$ ,  $(x^+ - L) = 0.034$ . The remainder can be approximated by

$$\begin{aligned}
 & x = 0.338 \\
 & \int_{0.304}^{x^+} = a + bx^+ \sum \frac{1}{\gamma_m^4(-H^i)} + b \sum \frac{1}{\gamma_m^6(-H^i)} - (a + bx^+ - 0.05 b) \\
 & \quad \sum \frac{e^{-0.05}}{\gamma_m^4(-H^i)} + b \sum \frac{e^{-0.05} \gamma_m^2}{\gamma_m^6(-H^i)} \quad \text{eq. 14}
 \end{aligned}$$

Since  $q$  is linear over this region then

$$q(L) = a + b L$$

Evaluated series is

$$\int_0^{x^+} = 0.3095(a + bx^+) - 0.00560 b - (a + bx^+ - 0.05 b)(0.03335) + 0.001093 b$$

eq. 15

at  $L = 0.338$

$$q(L) = 3.5$$

$L = 0.304$

$$q(L) = 3.1$$

solving  $3.5 = a + 0.338 b$

$$\underline{3.1 = a + 0.304 b}$$

$$a = -0.48$$

$$b = 11.8 L$$

$$q(L) = -0.48 + 11.8 L$$

eq. 16

on Sub. in eq. 15

$$\int_{0.304}^{0.334} = 0.3095 \left[ -0.48 + (11.8)(0.338) \right] - 0.00560(11.8) - \left[ -0.48 + 11.8(0.338) - 0.05(11.8) \right] \left[ 0.03335 \right] + 0.001093(11.8)$$

$$\int_{0.304}^{0.334} = \underline{0.93}$$

Simpson's Rule is used to evaluate the remaining integral

$$\int_0^{0.304} = \frac{0.034}{3} (0.496 + 4(1.57) + 5.50)$$

$$\int_0^{0.304} = \underline{0.139}$$

Then

$$\int_0^{0.338} -0.139 + 0.93 = 1.069$$

Sub eq. 13

$$Nu(x^+ = 0.338) = \frac{(2)(3.5) \times 10^{-5}}{1.069 \times 10^{-5}} = 6.55$$

$$\frac{Nu_x^+}{Nu_\infty} = \frac{6.55}{6.46} = 1.015$$

Since the Nusselt number for this run is 5.85, the corrected number is

$$Nu_c 1.015 \times 5.85 = 5.95$$

To avoid repetition in calculations the results of Run 11-2 are tabulated in Table 5.

Table 5 - Results Showing the Effect of Variable Heat Flux  
on the Local NaK Conductance - Run 11-2

x Inches of Annulus	x <sup>+</sup>	Nu <sub>x<sup>+</sup></sub> Nu <sub>∞</sub>	Corrected Nu Nu <sub>x<sup>+</sup></sub> x 5.85 Nu <sub>∞</sub>	Corrected Wall Temp. (°F)	Water Coefficients h <sub>reported</sub> Btu/hr sqft °F	h <sub>corrected</sub> Btu/hr sqft °F
6	0.338	1.015	5.95	1029	-	-
6.5	0.372	1.035	6.05	994	1,170	1,168
7.0	0.405	1.058	6.20	945	-	-
7.5	0.438	1.09	6.38	862	3,260	3,160
8.0	0.473	1.12	6.66	735	11,000	9,200
8.5	0.507	1.015	5.95	651	137,000	64,500

The various temperatures (Run 11-2) are plotted as a function of position along the tube, together (by a solid line) with the original inner tube wall temperatures calculated on the basis of an assumed constant NaK Nusselt number (see Fig. 10). It is apparent from the curve that the effect (axial variation of heat flux on NaK conductance) is very small, except for the region in the early partial film stage.

Table 5 also shows the magnitude of this effect (variable heat flux) on the water coefficients. This effect is only significant in the burnout region since this is the area of greatest heat flux change.

The results of the other three runs, which are similar to Run 1, are tabulated in Table 6. The runs show a difference in Nusselt number at peak flux changes as much as 17%. The significant error occurs in the vicinity of the peak heat flux region, where the tube wall temperature changes rapidly as film blanketing causes a reduction in the rate of heat transfer. Since the longitudinal temperature gradient of the NaK film is changing, the heat conducted longitudinally in the NaK film is also varying and affects the calculated values of Nusselt Number. This effect is of appreciable magnitude only in the burnout region where the heat flux changes rapidly. It is obvious from the table that this occurs over approximately 1/2 in. length of the tube. In conclusion, it is felt that the experimental error in this critical region is of such magnitude as to overshadow the effects suggested by Kays<sup>10</sup>.

The authors presented this analysis to show the possibility of error in the peak heat flux region. An attempt will be made in future tests to minimize the experimental error by incorporating additional thermocouples in the critical region.

Table 6 - Results on Corrected NaK Conductance

Run No.	Distance Along Annulus (in.)	Nusselt Number			$\% = \frac{Nu_{corr.} - Nu_{const.heat flux}}{Nu_{const.heat flux}} \times 100$	
		$Nu(x^+)$	Constant			
			Heat Flux	Corrected		
6-3	5	1.17	5.76	6.75	17.2	
	6	1.114	5.76	6.42	11.5	
	6.5	1.034	5.76	5.96	3.47	
	7	0.993	5.76	5.73	- 0.52	
-----						
7-1	3.5	1.05	5.54	5.83	5.2	
	4.5	1.07	5.54	5.93	7.04	
	5.5	1.142	5.54	6.33	14.25	
	6.5	1.07	5.54	5.93	7.04	
-----						
10-3	6	0.991	6.02	5.96	- 0.99	
	7	1.04	6.02	6.26	4.0	
	8	1.11	6.02	6.67	11.0	